

# Mapping genetic loci that regulate lipid levels in a NZB/B1NJ×RF/J intercross and a combined intercross involving NZB/B1NJ, RF/J, MRL/MpJ, and SJL/J mouse strains

Jon E. Wergedal,<sup>\*,†</sup> Cheryl L. Ackert-Bicknell,<sup>§</sup> Wesley G. Beamer,<sup>§</sup> Subburaman Mohan,<sup>\*,†</sup> David J. Baylink,<sup>\*</sup> and Apurva K. Srivastava<sup>1,\*,†</sup>

Musculoskeletal Disease Center,<sup>\*</sup> Loma Linda VA Health Care Systems, Loma Linda, CA; Department of Medicine,<sup>†</sup> Loma Linda University, Loma Linda, CA; and Jackson Laboratory,<sup>§</sup> Bar Harbor, ME

**Abstract** The NZB/B1NJ (NZB) mouse strain exhibits high cholesterol and HDL levels in blood compared with several other strains of mice. To study the genetic regulation of blood lipid levels, we performed a genome-wide linkage analysis in 542 chow-fed F2 female mice from an NZB×RF/J (RF) intercross and in a combined data set that included NZB×RF and MRL/MpJ×SJL/J intercrosses. In the NZB×RF F2 mice, the cholesterol and HDL concentrations were influenced by quantitative trait loci (QTL) on chromosome (Chr) 5 [logarithm of odds (LOD) 17–19; *D5Mit10*] that was in the region identified earlier in crosses involving NZB mice, but two QTLs on Chr 12 (LOD 4.7; *D12Mit182*) and Chr 19 (LOD 5.7; *D19Mit1*) were specific to the NZB×RF intercross. Triglyceride levels were affected by two novel QTLs at *D12Mit182* (LOD 8.7) and *D15Mit13* (LOD 3.5). The combined-cross linkage analysis (1,054 mice, 231 markers) identified four shared QTLs (Chrs 5, 7, 14, and 17) that were not detected in one of the parental crosses and improved the resolution of two shared QTLs. In summary, we report additional loci regulating lipid levels in NZB mice that had not been identified earlier in crosses involving the NZB strain of mice. The identification of shared loci from multiple crosses increases confidence toward finding the QTL gene.—Wergedal, J. E., C. L. Ackert-Bicknell, W. G. Beamer, S. Mohan, D. J. Baylink, and A. K. Srivastava. Mapping genetic loci that regulate lipid levels in a NZB/B1NJ×RF/J intercross and a combined intercross involving NZB/B1NJ, RF/J, MRL/MpJ, and SJL/J mouse strains. *J. Lipid Res.* 2007. 48: 1724–1734.

**Supplementary key words** high density lipoprotein cholesterol • cholesterol • triglyceride • quantitative trait loci • combined-cross linkage analysis

Cardiovascular disease is the leading cause of death and premature disability in the United States and other

industrialized countries (1, 2). Cardiovascular disease has a complex etiology, involving multiple genetic and environmental interactions (3, 4). Recognized risk factors include cholesterol and triglyceride levels, hypertension, obesity, diabetes, and the metabolic syndrome, all of which are complex traits with multiple genes involved in their regulation. Identification of the genes affecting susceptibility to cardiovascular disease has been a major undertaking for researchers, as earlier identification of the individuals predisposed to cardiovascular disease would maximize the gains from preventive interventions. To date, only a few genes that regulate blood levels of lipids have been identified (5–10).

Specifying a chromosomal locus is a necessary first step toward finding the genes that regulate lipid levels and identifying the causative molecular etiology. Inbred strains of mice have been used as a powerful tool to identify quantitative trait loci (QTL) contributing to variations in circulating levels of lipids (11–28). The QTL studies in mice have not only revealed a large number of loci regulating lipid levels in blood but have also shown that there is a high degree of concordance between human QTLs regulating lipid levels and corresponding mouse loci (26, 27). More than 10 different crosses have been used to map nearly 100 loci, distributed across all autosomes that regulate plasma lipid levels. However, only a small number of linkages have been identified in multiple crosses, indicating that we are limited to discovering only loci that show allelic variation between the strains used in a particular cross. By looking at additional crosses, we can sample more allelic variation; thus, we have an opportunity to detect additional loci that can be implicated in a disease model. In addition, combined analysis of data from multiple F2 crosses were recently suggested as a means to achieve

Manuscript received 10 January 2007 and in revised form 12 April 2007.  
Published, JLR Papers in Press, May 13, 2007.  
DOI 10.1194/jlr.M700015-JLR200

<sup>1</sup>To whom correspondence should be addressed.  
e-mail: apurva.srivastava@med.va.gov

greater sample size and power for detecting and localizing the QTLs (29–31). The combined analyses have also indicated increased resolution of the shared QTLs, which is major bottleneck in the ultimate goal of a QTL analysis: identification of the underlying gene (29). Therefore, the above rationale implies that the best estimate of the number and location of genes that account for the variation of lipid levels in mice can be achieved by comparing the results of multiple crosses.

We recently used the NZB/B1NJ (NZB) and RF/J (RF) mouse strains to identify linkage to several loci that specifically regulate bone size and mechanical properties (32). The NZB strain is known to have high total cholesterol (herein termed “cholesterol”) and high density lipoprotein cholesterol (herein termed “HDL”) concentrations in blood (11, 15, 17, 21); in contrast, the RF mouse strain has not been studied for lipid metabolism. Consequently, we took advantage of the availability of serum samples from NZB×RF F2 mice [designated (NZB×RF)F2] to map genetic loci that regulate lipid levels. We confirmed that chow-fed (diet with 4–6% fat content by weight) NZB and RF mice display significant differences in serum levels of cholesterol, HDL, and triglycerides. The aim of this study was to enumerate and map the genetic loci that regulate cholesterol, HDL, and triglyceride levels in (NZB×RF)F2 mice. An additional aim was to further analyze the (NZB×RF)F2 data by combining it with data from a previously published study (28) of a cross of MRL/MpJ (MRL) and SJL/J (SJL) mouse strains [designated (MRL×SJL)F2] using a recently suggested combined-cross analysis (29–31).

## MATERIALS AND METHODS

### Mice

All mice used in this study were maintained and housed in the accredited animal care facility at the Jackson Laboratory, and the study was performed according to approved procedures. Breeding of NZB and RF mice, generation of F1 and F2 progeny, collection of DNA samples, and collection and processing of blood have been described previously (32). In brief, NZB females were mated with male RF mice to produce F1 mice. Then, F1×F1 matings were established to produce F2 mice. Only female F2 mice were weaned onto a 4% fat diet (5K54; LABDIET, St. Louis, MO) at 21 days and housed three to six animals per cage. All mice were allowed free access to food and water throughout the course of the study. Mice were euthanized at 10 weeks of age by decapitation at the same time of day (between 9:00 AM and noon) under nonfasting conditions. Whole blood was collected and clotted on ice for 1 h and subsequently spun down in a microcentrifuge. Serum was removed to a clean plastic tube and stored at  $-20^{\circ}\text{C}$  until it was shipped to the VA Loma Linda for analysis (where serum was stored at  $-70^{\circ}\text{C}$  until analysis).

### Serum cholesterol, HDL, and triglyceride measurements

Cholesterol, HDL, and triglyceride were measured by direct enzymatic colorimetric assays using a fully automated Hitachi 912 Clinical Chemistry analyzer (Roche, IN) as described previously (28). Serum samples from previously reported (MRL×SJL)F2

mice (28) were analyzed on the same instrument under identical conditions with the same lot of reagents used in this study.

### Construction of the linkage map

The extraction of genomic DNA and PCR-based genotyping with 94 microsatellite markers covering 19 autosomes have been described previously (32). The order of genetic markers was obtained for each chromosome (Chr) from the publicly available Mouse Genome Informatics database (MGI 3.51; <http://www.informatics.jax.org/>).

### Statistical analysis

The phenotype data were analyzed using GraphPad Prism (Windows version 4.02; GraphPad Software, San Diego, CA). The Shapiro-Wilk test was used to test the normality of phenotypic data from F2 mice. One-way ANOVA with Newman-Keuls test was used to compare pairs of data to determine statistically significant differences in plasma lipid levels between mouse strains. The genotype data were analyzed using the Pseudomarker MAINSCAN algorithm written for the MATLAB (Mathworks, Inc., Natick, MA) programming environment (28, 33). Threshold values for significant LOD scores for different QTLs were determined by genome-wide 1,000 permutation tests for 5% genome-wide error ( $P < 0.05$ ). The 95% confidence intervals (CIs) were derived from posterior probability plots for individual Chrs as described previously (28). Linkage analyses were also performed using MapQTL 5.0 (DLO) Center for Plant Breeding and Reproduction Research, Wageningen, The Netherlands) as described for F2 intercrosses. Both Pseudomarker and MapQTL 5.0 analyses yielded very similar results. The percentage variance explained by each locus was calculated for peak intervals by MapQTL software. A genome-wide search for epistasis was performed with the Pseudomarker PAIRSCAN algorithm as described previously (28, 33, 34).

### Genome-wide linkage analysis using data from combined crosses

Finding repetitive QTLs in crosses with different strains suggests that they may have arisen from shared ancestral alleles. We combined the data from (NZB×RF)F2 mice in this report with data from (MRL×SJL)F2 mice reported recently (28). Alleles were recoded based on the progenitor strain phenotype shown in Fig. 1D, and we combined the raw data by recording NZB and MRL genotypes as high HDL alleles and SJL and RF genotypes as low HDL alleles. The genetic map and positions of 231 markers used in this study were implemented from MGI 3.51. For identical markers (14), genotype and phenotype data were merged. Genome-wide scans and calculation of significance values were performed as described previously (29–31).

## RESULTS

### Serum lipoprotein and cholesterol profiles of NZB, RF, F1, and (NZB×RF)F2 intercross mice

Examination of serum lipid levels demonstrated substantial differences between NZB and RF mice. The cholesterol and HDL values were 48% ( $P < 0.001$ ) and 57% ( $P < 0.001$ ) higher in NZB mice compared with RF mice (Fig. 1A, C), respectively. The triglyceride levels were 58% ( $P < 0.001$ ) higher in RF mice compared with NZB mice (Fig. 1B). At 10 weeks of age, the RF mice had 10% ( $P < 0.05$ ) higher body weight compared with NZB mice

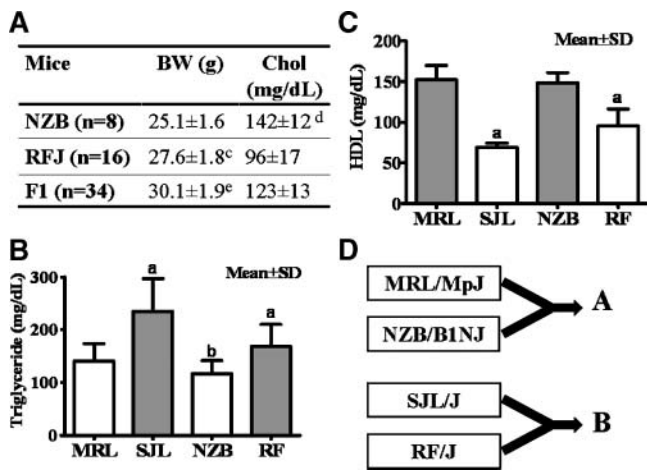


**Fig. 1.** Encoding alleles of genotype data from the (NZB×RF)F2 intercross (data from this study) and the (MRL×SJL)F2 intercross (29) for combined-cross analysis of genome-wide linkages. **A:** Body weight (BW) and triglyceride levels (means ± SD) in NZB/B1NJ (NZB), RF/J (RF), and NZB×RF F1 (F1) mice. **B:** Triglyceride levels were higher in RF and SJL/J (SJL) strains of mice. **C:** HDL (and total cholesterol) levels were higher in NZB and MRL/MpJ (MRL) strains of mice. **D:** Based on the phenotype, NZB and MRL genotypes were denoted allele A and RF and SJL genotypes were denoted allele B. *P* values are as follows: <sup>a</sup> *P* < 0.05 versus MRL and NZB; <sup>b</sup> *P* > 0.05 versus MRL; <sup>c</sup> *P* < 0.05 versus NZB; <sup>d</sup> *P* < 0.05 versus RF and F1; <sup>e</sup> *P* < 0.05 versus NZB and *P* > 0.05 versus RF. All *P* values were calculated by ANOVA.

(Fig. 1A). In (NZB×RF)F2 female mice, there was a highly significant correlation between body weight and cholesterol (Pearson  $r = 0.65$ ,  $P < 0.001$ ), HDL ( $r = 0.64$ ,  $P < 0.001$ ), and triglycerides ( $r = 0.2$ ,  $P < 0.001$ ). The cholesterol ( $96 \pm 17$  mg/dl) and HDL ( $95 \pm 21$  mg/dl) levels (mean ± SD) were intermediate and significantly different in F1 mice ( $P < 0.01$  by ANOVA) compared with those of the parental strains. The triglyceride levels in F1 mice ( $169 \pm 41$  mg/dl) were significantly higher than in NZB mice but comparable to those of RF mice ( $P > 0.05$  by ANOVA).

In (NZB×RF)F2 mice, the distributions of cholesterol, HDL, and triglyceride ( $207 \pm 75$  mg/dL) did not pass the normality test (Shapiro Wilk  $W = 0.95$ – $0.98$ ,  $P < 0.01$ ). Consequently, all lipid data were converted into log values before QTL analysis, and log-transformed data are shown in **Figs. 2–4** (one extreme outlier was deleted from the triglyceride data analysis). The log-transformed lipid values were normally distributed (Shapiro Wilk,  $P > 0.05$ ,  $n = 542$ ). As expected for chow-fed mice, there was a highly significant correlation between cholesterol and HDL levels in the F2 mice ( $n = 542$ ,  $r = 0.96$ ,  $P < 0.0001$ ). Cholesterol levels showed a low but highly significant positive correlation with triglyceride levels ( $r = 0.2$ ,  $P < 0.001$ ). The range of F2 values exceeded mean ± 2 SD parental intervals for each trait. Together, these data suggest a complex inheritance of serum lipid levels in this cross.

#### Localization of cholesterol, HDL, and triglyceride QTLs

Although genotype data for 737 (NZB×RF)F2 female mice were available, the linkage maps for lipids were gen-

erated using a subgroup of 542 F2 mice for which blood was available (some blood samples could not be collected or were lost during shipment). The results of interval mapping of these traits are shown in **Figs. 2–4**. Three statistically significant cholesterol QTLs were identified on Chrs 5, 12, and 19 (**Table 1**). The highest LOD score was observed for the Chr 5 locus with a peak LOD score of 16.7 at marker *D5Mit10* (**Fig. 3**). As expected for chow-fed mice, the HDL loci were coincident with loci underlying cholesterol levels (**Figs. 2, 3**). QTLs on Chr 5 exerted the strongest effect on cholesterol and HDL, explaining ~17% and 18% of the variance in (NZB×RF)F2 mice. Detailed maps of each of the HDL loci and their 95% CI are shown in **Fig. 5A–C**. Significant linkages for triglyceride were observed on two loci located on Chrs 12 and 15 (**Figs. 4, 6**). **Figure 6A, B** shows the 95% CI for loci on Chrs 12 and 15. Together, these two loci explain ~15% of the F2 variance in triglyceride levels, indicating that additional linkages are likely involved that were not detected in this study despite the large number of F2 mice analyzed.

Consistent with low levels of non-HDL cholesterol in (NZB×RF)F2 mice ( $4.07 \pm 0.23$  mg/dl), we did not observe any significant LOD scores for non-HDL cholesterol.

#### Allelic variation for QTLs affecting lipid levels in (NZB×RF)F2 mice

To examine the mode of inheritance, mean values of lipid phenotypes for mice that are homozygous or heterozygous were determined at peak marker locations. In addition, to evaluate the location of the QTLs, posterior probability density plots were generated for each QTL. The results of these analyses are given in **Figs. 5, 6**. At the peaks of linkage for HDL and TG, the phenotypic means in (NZB×RF)F2 mice represented by the closest markers are shown in **Figs. 5D–F** and **6C, D**, respectively. The genetic allele distributions of peak markers for cholesterol QTLs were similar to those for HDL QTLs (data not shown). At the Chr 12 locus, the mean HDL levels for the homozygous NZB alleles were 9% higher than homozygotes for RF alleles ( $P < 0.01$ ) (**Fig. 5D**), and the phenotypic effect of the NZB allele best fits a dominant model. For the loci on Chr 19, homozygotes for the RF allele had 12% ( $P < 0.001$ ) lower HDL levels (**Fig. 5E**) than the homozygotes for the NZB allele. The phenotypic effect for the NZB allele best fit a recessive mode of inheritance. For the QTL on Chr 5, the homozygotes for the NZB allele had 23% ( $P < 0.0001$ ) higher HDL compared with the homozygotes for the RF allele (**Fig. 5F**), and the phenotypic effect of the NZB allele best fits an additive model.

For QTLs regulating triglyceride levels (**Fig. 6A, B**), the phenotypic effects of the Chr 12 allele for homozygotes of NZB alleles were 28% higher than those for the homozygotes of RF alleles (**Fig. 6C**). The NZB alleles appear to be inherited in an additive manner. For QTLs identified on Chr 15, the homozygotes for RF alleles had 14% ( $P < 0.01$ ) higher triglyceride levels compared with NZB homozygotes and appeared to be inherited in a recessive manner (**Fig. 6D**).

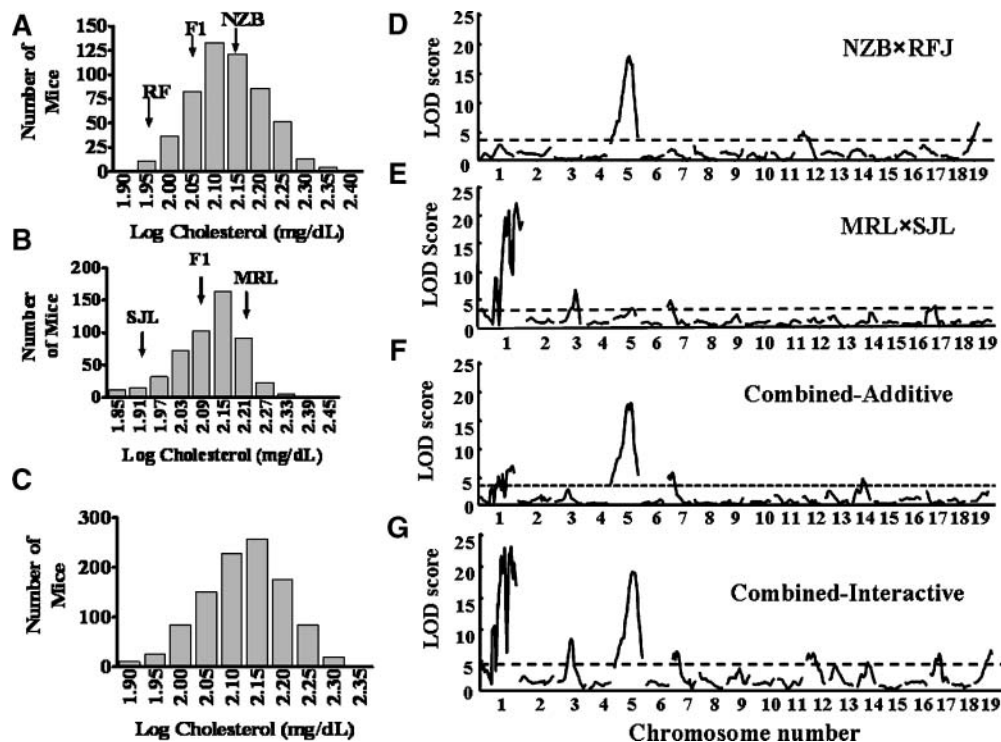


**Fig. 2.** Genome-wide linkage map of cholesterol levels in (NZB×RF)F2 female mice and combined-cross analysis. A–C: Distribution of log-transformed cholesterol levels in (NZB×RF)F2 mice (A), (MRL×SJL)F2 mice (B), and combined F2 data (C). D, E: Whole genome linkage maps of cholesterol in (NZB×RF)F2 mice (D) and (MRL×SJL)F2 mice (E). F, G: Genome-wide linkage maps in combined-cross analysis. Combined-additive indicates quantitative trait loci (QTLs) detected using cross as an additive covariate, and combined-interactive indicates QTLs detected using cross as an interactive covariate. The horizontal dotted lines in D–G indicate the threshold for genome-wide significance ( $P < 0.05$ ).

Although the triglyceride levels were higher in the RF strain compared with the NZB strain of mice (Fig. 1B), it is noteworthy that for the Chr 12 QTL, the homozygotes for NZB alleles accounted for higher triglyceride levels. Similar retrogressive QTLs have been observed in other QTL analyses (35).

#### QTL-QTL interactions

The LOD scores for all locus interactions, determined using the Pseudomarker PAIRSCAN software program, were moderate and mainly suggestive in nature (data not shown) for the (NZB×RF)F2 cross.

#### Combined-cross genome-wide linkage analysis

With the increased power of the combined-cross analysis, we detected a significantly higher number of loci for cholesterol, HDL, and triglyceride levels compared with those observed in the individual (MRL×SJL)F2 and (NZB×RF)F2 crosses. Detailed LOD score plots for “cross” as an additive or interactive covariate are given in Figs. 2–4, and LOD scores are shown in **Table 2**. In addition to the QTLs identified in (NZB×RF)F2 mice, new QTLs on Chrs 14 and 17 were discovered in the combined-cross analysis. The LOD score difference between additive and interactive analysis exceeded the significant threshold for loci on Chrs 1, 3, 12, and 19. Thus, these loci were

cross-specific. Linkages identified on Chrs 5, 7, 14, and 17 were shared between the (NZB×RF)F2 and (MRL×SJL)F2 crosses. Contrary to combined-cross analysis results, loci on Chrs 7 and 14 did not reach statistical significance in the (NZB×RF)F2 cross.

The Chr 5 QTL regulating HDL levels in (NZB×RF)F2 progeny was identified as a shared QTL in the combined-cross analysis. This QTL is concordant with that reported previously in (MRL×SJL)F2 mice (28) and (NZB×SM)F2 and (NZB×B6)F2 mice (12, 21). The LOD score of this shared QTL was increased in combined-cross analysis (LOD 22.8), and resolution of this QTL was improved slightly [95% CI decreased to 56–64 centimorgan (cM)] (Fig. 7A). The allele distribution for HDL values at the Chr 5 peak (Fig. 7C) shows that homozygotes for allele A contribute 19% higher HDL ( $P < 0.001$ ) levels compared with those for allele B (details of the alleles are shown in Fig. 1D). Our results, using a statistical analysis described previously (30), demonstrated that the Chr 5 QTL represents a single QTL.

Linkages that regulate triglyceride levels in combined-cross analysis were mainly cross-specific, as shown in Table 2. The Chr 12 QTL regulating triglyceride levels was observed in both (NZB×RF)F2 and (MRL×SJL)F2 crosses but was lost in the combined additive analysis (Table 2). Consequently, we recoded the NZB and MRL genotypes

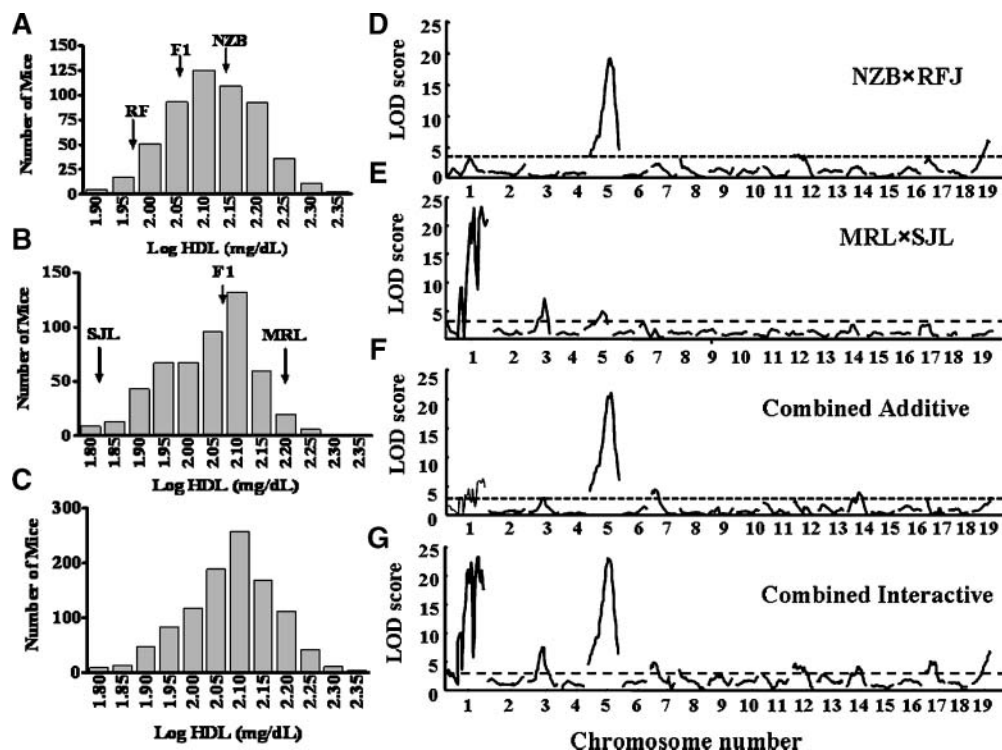


**Fig. 3.** Genome-wide linkage map of HDL levels in (NZB×RF)F<sub>2</sub> female mice and combined-cross analysis. A–C: Distribution of log-transformed HDL levels in (NZB×RF)F<sub>2</sub> mice (A), (MRL×SJL)F<sub>2</sub> mice (B), and combined F<sub>2</sub> data (C). D, E: Whole genome linkage maps of cholesterol in (NZB×RF)F<sub>2</sub> mice (D) and (MRL×SJL)F<sub>2</sub> mice (E). F, G: Genome-wide linkage maps in combined-cross analysis. Combined-additive indicates QTLs detected using cross as an additive covariate, and combined-interactive indicates QTLs detected using cross as an interactive covariate. The horizontal dotted lines in D–G indicate the threshold for genome-wide significance ( $P < 0.05$ ).

as a high triglyceride allele and the RF and SJL genotypes as a low triglyceride allele. Reanalysis of the Chr 12 data showed a highly significant QTL with a LOD score of 10.14 (95% CI limits of 0–13 cM), which is shared between (NZB×RF)F<sub>2</sub> and (MRL×SJL)F<sub>2</sub> crosses. The posterior probability density plot of the Chr 12 QTL strongly suggests the presence of two distinct peaks (Fig. 7B). The 95% CI for proximal and distal peaks corresponded to 0–12 cM and 29–34 cM, respectively (Fig. 7A). The allele distribution for peak markers *D12Mit182* and *D12Mit201*, which are used in both (NZB×RF)F<sub>2</sub> and (MRL×SJL)F<sub>2</sub> crosses, are shown in Fig. 7D, E. Thus, the combined-cross analysis further clarifies the identification of two triglyceride peaks on Chr 12.

## DISCUSSION

In this study, we expand the current knowledge about loci regulating lipid levels by using a large number of female F<sub>2</sub> mice generated from a new intercross involving NZB and RF inbred strains. The genome-wide analyses of (NZB×RF)F<sub>2</sub> mice resulted in the localization of three significant QTLs for cholesterol and HDL and two significant QTLs regulating triglycerides. By combining the (NZB×RF)F<sub>2</sub> cross with a previously published (MRL×SJL)F<sub>2</sub> cross, three additional loci were identified on Chrs

7, 14, and 17 that regulate HDL and cholesterol levels. Of three loci (Chrs 5, 12, and 19) that regulate HDL and cholesterol levels, two QTLs on Chrs 12 and 19 are specific to the (NZB×RF)F<sub>2</sub> cross and were not detected in any of the earlier crosses involving the NZB strain of mice (11, 12, 16, 21, 25, 26). Thus, the Chr 12 and 19 QTLs represent novel linkages that regulate HDL levels in NZB mice. The strongest linkage for cholesterol and HDL was identified on Chr 5 in (NZB×RF)F<sub>2</sub> mice. The location and peak of only this locus is concordant with linkage identified previously in both chow-fed and atherogenic diet-fed F<sub>2</sub> mice from (NZB×SM)F<sub>2</sub> and (B6×CAST/Ei)F<sub>2</sub> crosses (11, 12, 16, 21, 25, 26). However, the posterior density plot (Fig. 7) localized the 95% CI to a narrower interval (54–66 cM) compared with the concordant linkages identified in (NZB×SM)F<sub>2</sub> crosses reported earlier (11, 12, 16, 21, 25, 26). A concern in the present (NZB×RF)F<sub>2</sub> cross was that the combined effect of QTLs accounts for only 30% of the total variance in cholesterol and HDL levels, suggesting that additional linkages are involved but were not detected. Possibly, the assay noise obscured the detection of small effect modifiers. In addition, the best estimate of total variance explained is obtained by identifying pleiotropic interactions (36), which is a challenging task because of a lower power to detect such interactions. In this study, we only observed weak interactions (data not shown),

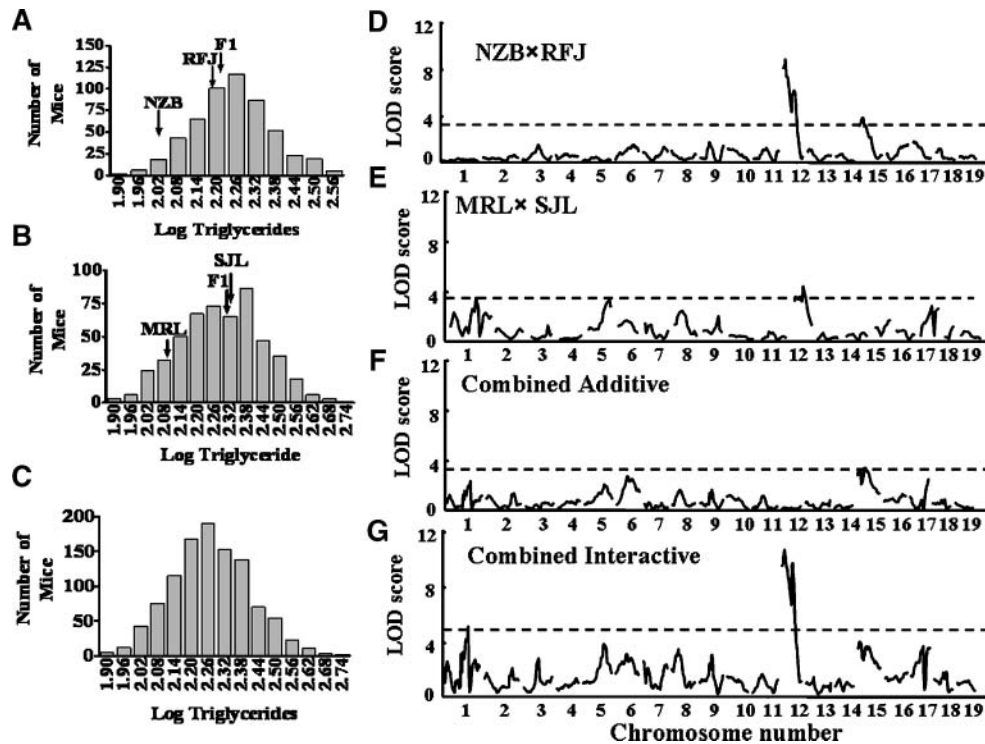


**Fig. 4.** Genome-wide linkage map of triglyceride levels in (NZB×RF)F2 female mice and combined-cross analysis. A–C: Distribution of log-transformed triglyceride levels in (NZB×RF)F2 mice (A), (MRL×SJL)F2 mice (B), and combined F2 data (C). D, E: Whole genome linkage maps of cholesterol in (NZB×RF)F2 mice (D) and (MRL×SJL)F2 mice (E). F, G: Genome-wide linkage maps in combined-cross analysis. Combined-additive indicates QTLs detected using cross as an additive covariate, and combined-interactive shows QTLs detected using cross as an interactive covariate. The horizontal dotted lines in D–G indicate the threshold for genome-wide significance ( $P < 0.05$ ).

which may partly explain the low percentage variance represented by the loci identified in this study.

Our findings on the Chr 5 QTL region reaffirm that this locus is a strong candidate for positional and molecular cloning. To identify candidate genes, we searched the MGI 3.51 database and located 75 transcripts showing single-nucleotide polymorphisms between NZB and RF strains of mice. Prominent candidates included the following: 1) ATP binding cassette, subfamily G, member 3 (*Abcg3*) (Chr 5, 59 cM); the protein encoded by this gene is a

member of the superfamily of ATP binding cassette transporters involved in the regulation of lipid-trafficking mechanisms (37); 2) leucine-rich repeat-containing 8 family, member C (*Lrrc8c*), which has a role in regulating adipocyte differentiation (38); 3) diacylglycerol kinase, theta (*Dgkq*) (Chr 5, 57 cM), which is involved in glycerophospholipid metabolism (39); 4) Hermansky-Pudlak syndrome 4 homolog (human) (*Hps4*) (Chr 5, 59 cM); homozygotes for a spontaneous null mutation for *Hps4* exhibit resistance to diet-induced atherosclerosis (40); 5) mevalonate

**TABLE 1.** Significant QTLs that influence lipid levels in chow-fed female (NZB×RF)F2 mice

Phenotype	Chr	Peak Marker	95% Confidence Interval		LOD Score <sup>a</sup>	P	Variance Explained
			cM	cM			by Peak Interval
							%
Cholesterol	5	58		53–64	17.63	<0.000001	17.0
	12	14		0–24	4.85	0.000022	6.3
	19	48		42–52	6.29	<0.000001	6.2
HDL	5	56		55–66	18.3	<0.000001	18.7
	12	14		0–30	3.57	0.000269	5.3
Triglyceride	19	49		40–52	5.56	0.000003	5.6
	12	8		0–30	8.66	<0.000001	10.9
	15	2		0–25	3.46	0.000348	4.4

Chr, chromosome; QTL, quantitative trait locus.

<sup>a</sup>The cutoff for significant QTLs for genome-wide significance calculated for  $P < 0.05$  was LOD 3.2 for cholesterol and HDL and LOD 3.1 for triglyceride levels.

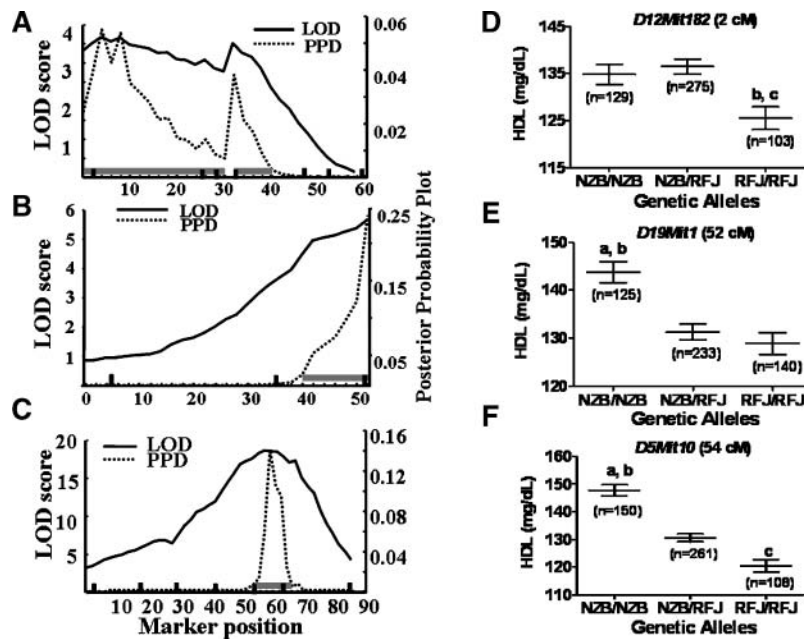


**Fig. 5.** A–C: LOD score and posterior probability density (PPD) plots for the three significant QTLs on chromosomes (Chrs) 12, 19, and 5 that influence HDL levels in the (NZB×RF)F<sub>2</sub> mice. Locations of the markers are shown as thick vertical lines on the x axis. Posterior probability density is a likelihood statistic that gives rise to the 95% confidence intervals (CIs), indicated by gray horizontal bars. D–F: Allelic contribution of the closest marker located on corresponding QTL peaks. NZB/NZB represents homozygosity for NZB alleles, RF/RF represents homozygosity for RF alleles, and heterozygosity at a locus is represented by NZB/RF. Error bars represent SEM. <sup>a</sup>  $P < 0.05$  versus RF/RF; <sup>b</sup>  $P < 0.05$  versus NZB/RF; <sup>c</sup>  $P < 0.05$  versus NZB/NZB and NZB/RF (by ANOVA). cM, centimorgan.

kinase (*mk*) (Chr 5, 64 cM), a gene involved in cholesterol biosynthesis (41); and 6) glycerol kinase 2 (*Gk2*) (Chr, 53 cM), a gene involved in glycerolipid metabolism (42).

Previous data published by our laboratory on the (NZB×RF)F<sub>2</sub> mice (32) indicated that the Chr 5 (LOD 4.7, 50 cM) locus was colocalized with a locus that regulates bone geometry. There could be some concordance between the genetic regulation of bone phenotype and HDL level, because circulating lipid levels are believed to be a risk factor that affects skeletal phenotype. Consistent with

this observation, Ishimori et al. (43) recently reported common linkage that regulates bone mineral density and lipid levels. Two QTLs observed in (NZB×RF)F<sub>2</sub> mice colocalized with body weight QTLs: the Chr 12 locus (body weight QTL LOD 14.7, 2.0 cM) and the Chr 19 locus (body weight QTL LOD 5.2, 50 cM). Increased body weight as a function of QTLs on Chr 12 and 19 is contributed by NZB alleles. Although we observed a strong correlation between HDL levels and body weight in (NZB×RF)F<sub>2</sub> mice, it remains to be verified whether the effects of Chr 12 and

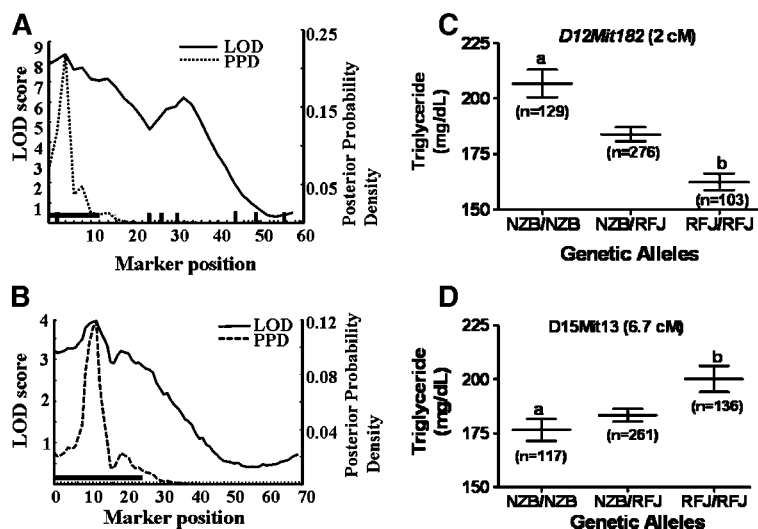


**Fig. 6.** A, B: LOD score and posterior probability density (PPD) plots for the two significant QTLs on Chrs 12 and 15 that influence triglyceride levels in the (NZB×RF)F<sub>2</sub> mice. Locations of the markers are shown as thick vertical lines on the x axis. Posterior probability density is a likelihood statistic that gives rise to the 95% CIs, indicated by gray horizontal bars. C, D: Allelic contribution of the closest marker located on corresponding QTL peaks. NZB/NZB represents homozygosity for NZB alleles, RF/RF represents homozygosity for RF alleles, and heterozygosity at a locus is represented by NZB/RF. Error bars represent SEM. <sup>a</sup>  $P < 0.05$  versus RF/RF; <sup>b</sup>  $P < 0.05$  versus NZB/RF (by ANOVA).

TABLE 2. Chromosomal loci identified in the combined-cross analysis of combining data sets from the (NZB×RF)F<sub>2</sub> mice and the previously reported (MRL×SjL)F<sub>2</sub> mice (28)

Chr	(NZB×RF)F <sub>2</sub>		(MRL×SjL)F <sub>2</sub>		Combined-Cross (Additive)		Combined-Cross (Interactive)	
	Peak	LOD Score <sup>a</sup>	Peak	LOD Score <sup>a</sup>	Peak	LOD Score <sup>b</sup>	Peak	LOD Score <sup>c</sup>
	<i>cM</i>		<i>cM</i>		<i>cM</i>		<i>cM</i>	
Cholesterol								
1			95	22.00	106	6.35	96	22.87
3			40	6.61	44	(2.81)	42	8.26
5	58	17.63	50	3.32	62	17.1	56	18.88 <sup>d</sup>
7			10	4.74	14	5.60	12	6.18 <sup>d</sup>
12	14	4.85					22	5.98
14					34	4.10	34	4.52 <sup>d</sup>
17					2	(2.47)	28	5.90
19	48	6.29			54	(2.57)	52	6.39
HDL								
1			95	23.20	106	6.20	96	23.08
3			40	7.02	44	2.89	42	7.40
5	60	16.95	45	4.86	62	20.92	56	22.8 <sup>d</sup>
7			10	2.95	12	4.32	12	4.77 <sup>d</sup>
12	12	4.66					8	4.51
14					34	3.81	34	4.05 <sup>d</sup>
17					2	(2.77)	18	4.94
19	48	5.66			54	3.03	52	6.69
Triglyceride								
1			76.2	3.80			76	5.06
12	8	8.66	26	4.10		— <sup>e</sup>	8	9.99
15	2	3.46			24	3.38		

<sup>a</sup>LOD scores are above the suggestive cutoff ( $P < 0.1$ ).

<sup>b</sup>LOD thresholds for suggestive ( $P < 0.1$ ) and significant ( $P < 0.05$ ) QTLs were 2.9 and 3.2, respectively, for both cholesterol and HDL. LOD thresholds for triglyceride were 3.0 ( $P < 0.1$ ) and 3.3 ( $P < 0.05$ ). LOD scores in parentheses were below, but close to, the suggestive threshold.

<sup>c</sup>LOD thresholds for suggestive ( $P < 0.1$ ) and significant ( $P < 0.05$ ) QTLs were 3.9 and 4.2, respectively, for cholesterol and HDL. LOD thresholds for triglyceride were 4.4 ( $P < 0.1$ ) and 4.8 ( $P < 0.05$ ).

<sup>d</sup>Defined as statistically significant shared QTLs (based on the difference between LOD scores obtained from combined-additive and combined-interactive).

<sup>e</sup>The combined-additive analysis showed a nonsignificant LOD score for the Chr 12 QTL when the NZB allele was coded as A, but a LOD score of 10.14 was observed when the NZB allele was recoded as B.

19 QTLs on body weight are related to higher HDL levels of NZB mice.

The 95% CI for the Chr 12 QTL regulating HDL levels was too large; therefore, a search for a candidate gene was unreasonable. For the Chr 19 QTL regulating HDL levels, we observed 30 transcripts showing polymorphisms between NZB and RFJ strains of mice (95% CI 40–50 cM). However, none of these transcripts represented any obvious candidates for this QTL. Notable candidates for which single-nucleotide polymorphisms are unknown between NZB and RFJ strains include the following: 1) stearoyl-CoA desaturase 1 and 2 (*Scd1*, *Scd2*) (Chr 19, 43 cM), genes that are involved in fatty acid and lipid biosynthesis (44); 2) phosphatidylinositol 4-kinase type 2 $\alpha$  (*Pi4k2a*) (Chr 19, 47 cM), which has lipid kinase activity (45); 3) carboxypeptidase N, polypeptide 1 (*Cpn1*) (Chr 19, 47 cM), which encodes a protein that has carboxypeptidase activity (45); 4) elongation of very long-chain fatty acids (*Elovl3*) (Chr 19, 47 cM); *Elovl3* null mice have abnormal hair lipid content with high levels of eicosenoic acid (46); 5) glycerol-3-phosphate acyltransferase (*Gpam*) (Chr 19, 52 cM), which regulates cellular lipid metabolic processes and fatty acid metabolism (47); and 6) acyl-CoA synthetase long-chain family member 5 (*Acs15*), which has catalytic activity for fatty acid metabolic processes (45).

The process of identifying genes for QTLs discovered to date has been slow because fine-mapping a biologically variable phenotype to a QTL region and narrowing the list of candidate genes in a QTL represents a challenging task. With >100 loci known to regulate HDL levels, the interest in fine-mapping the most important QTL will likely focus on repetitive linkages identified in multiple crosses (26). In this regard, combined-cross analysis has been suggested as a tool to identify repetitive QTLs and also to increase the resolution of closely associated QTLs (30, 31, 43). The underlying reasons are increased marker density, and the impact of combining the F<sub>2</sub> data is equivalent to that of adding more recombination events in the QTL region by using additional mice in a cross. As anticipated, the combined-cross analysis revealed higher numbers of QTLs that regulate cholesterol and HDL levels. The relevance of these QTLs is supported by their demonstration in several independent crosses reported previously (11, 12, 16, 21, 25, 26). Shared loci identified in the combined cross were located on Chrs 5, 7, 12, and 14 (Table 2). The Chr 7 QTL (95% CI 8–20 cM) regulating HDL levels includes three previously reported QTLs, *Hdl38* (48), *Lprq5* (11), and *Nhd1q6* (15), which regulate HDL or cholesterol levels. Two obvious candidates, nuclear receptor subfamily 1 group H, member 2 (*Nr1 h2*) (49) and platelet-activating



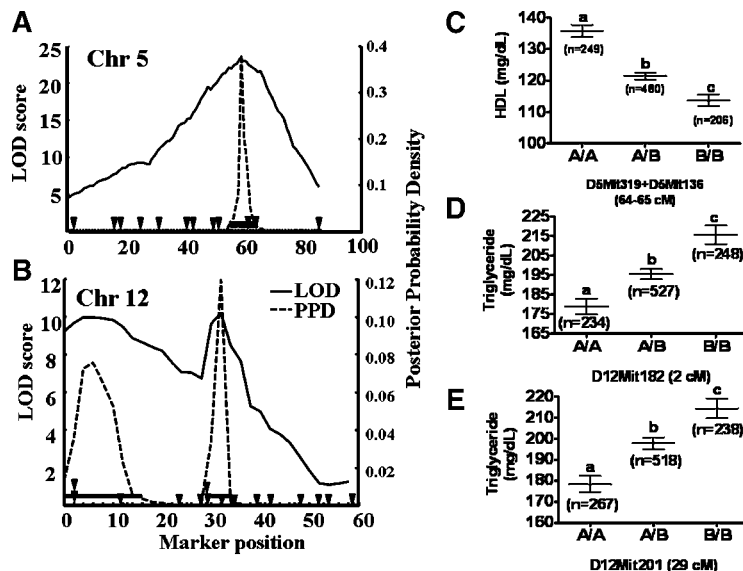


**Fig. 7.** Effect of combined-cross analysis on the resolution of QTLs. Data from (NZB×RF)F<sub>2</sub> and (MRL×SJL)F<sub>2</sub> intercrosses were combined to calculate the 95% CIs. A: The combined-cross analysis marginally improved the 95% CI of Chr 5 QTL (56–64 cM) regulating HDL levels. B: The posterior probability density (PPD) plot of combined-cross data resolved the Chr 12 QTL into two distinct linkages: a proximal peak with 95% CI of 0–13 cM and a distal peak with 95% CI of 29–34 cM. The approximate positions of markers are indicated on the x axis by inverted triangles; for markers that were merged, two triangles are shown one atop the other. C: Allele distribution of two peak markers, *D5Mit136* and *D5Mit319*, merged together showing that the combined effect of NZB and MRL alleles (represented as A) resulted in 19% higher HDL levels compared with those of RF and SJL (represented as B). D, E: Allele distribution of two markers, *D12Mit182* and *D12Mit201*, which were used in both NZB×RF and MRL×SJL F<sub>2</sub> intercrosses. Alleles were recoded for this analysis; therefore, allele A represents strains RF and MRL and allele B represents strains SJL and NZB. Error bars represent SEM. <sup>a,b,c</sup> *P* < 0.01 versus all other groups by ANOVA.

factor acetylhydrolase isoform 1b  $\alpha$ 1 subunit (*Pafah1b3*) (50), involved in lipid metabolism, are located within the Chr 7 QTL region. The Chr 14 QTL identified in the combined-cross analysis is a distinct linkage finding, with a 95% CI of 28–42 cM. We were unable to locate any obvious candidates for the Chr 14 QTL. In summary, the results of our combined-cross analysis revealed additional loci that are good candidates for positional cloning. However, the relevance of these QTLs remains to be validated by other means.

Among the QTLs that regulate triglyceride levels in both (NZB×RF)F<sub>2</sub> and (MRL×SJL)F<sub>2</sub> progeny, the locus on Chr 12 was most significant. Unexpectedly, this QTL was lost in the combined-cross analysis (Fig. 4, Table 2). Close examination of the allelic effects of the Chr 12 locus indicated that the coding strategy (Fig. 1D) used for combining the genotypes needs to be reversed because, in contrast to the low systemic triglyceride levels in NZB mice, F<sub>2</sub> mice homozygous for NZB alleles accounted for 12% (*P* < 0.01 by ANOVA) higher triglyceride levels compared with those for RF alleles (Fig. 6). Recoding of alleles resolved this artifact and revealed two distinct linkages (Fig. 7B). Thus, combined-cross analysis identified additional fractions of alleles that contribute to the genetic regulation of triglyceride levels. We believe that, in addition to the increased F<sub>2</sub> population size, the failure to detect two QTLs in individual crosses could be attributable

to a lack of marker coverage in this region of Chr 12. The proximal Chr 12 QTL (Fig. 7B) is a distinct linkage finding, with 95% CI representing a 0–13 cM region. This region harbors two important genes, apolipoprotein B (*ApoB*), which was located at 2.0 cM, and lipin-1 (*Lpin1*), which is located at 9 cM. Mutations of *ApoB*, which impair hepatic lipid export, are associated with fatty liver. *Lpin1* regulates lipid metabolism and fat cell differentiation. The homozygote for a spontaneous mutation in *Lpin1* (*Lpin1<sup>fld</sup>*) (51) mice has abnormalities in fat metabolism, increased serum and hepatic triglycerides, a liver-specific increase in mRNAs for apolipoproteins A-IV and C-II, and reduced apolipoprotein lipase activity in white adipose tissue (52). The distal Chr 12 QTL is in close proximity to an adiposity QTL (*Adip16*) and the atherosclerotic lesion area QTL (*Ascla6*). This region harbors a potential candidate gene, phosphatidylinositol glycan anchor (*Pigh*). It has been shown that lipoprotein lipase with a glycosylphosphatidylinositol anchor on cardiomyocytes develops lipotoxic cardiomyopathy associated with an increased cardiac uptake of plasma lipids (53); thus, it could be involved in triglyceride metabolism. Because our estimate of single-nucleotide polymorphisms between NZB and RF mouse strains is based on low-density single-nucleotide polymorphism listings, which are incomplete for several loci, our presumption regarding candidate genes for various QTLs

should be interpreted cautiously. Further confirmation will be required to substantiate these genes as bona fide candidates.

In conclusion, we have identified distinct linkages on Chrs 12, 19, and 15 regulating serum cholesterol, HDL, and triglyceride levels that were specific to the (NZB×RF)F<sub>2</sub> cross and confirmed the presence of several loci that were identified in previous genetic crosses involving the NZB strain of mouse. The combined-cross analysis revealed a large fraction of shared QTLs and improved resolution of the concordant QTLs to help prioritize potential candidate genes. Finally, our findings provide a strong rationale for finding the causative molecular etiology underlying loci on Chrs 5, 12, and 19. ■

This work was supported by the following grants from the National Institutes of Health: AR-46204 (J.E.W.) and AR-43618 (W.G.B.). Support was also provided by Army Assistance Award DAMD17-99-1-9571. The U. S. Army Medical Research Acquisition Activity (Fort Detrick, MD) is the awarding and administering acquisition office for the DAMD award. The information contained in this publication does not necessarily reflect the position or the policy of the U. S. Government, and no official endorsement should be inferred. All work was performed in facilities provided by the Department of Veterans Affairs or the Jackson Laboratory. The authors thank Aurora Petrilla for her excellent technical support.

## REFERENCES

1. American Heart Association. 2003. Heart and Stroke Statistics: 2003 Update. American Heart Association, Dallas, TX.
2. National Center for Health Statistics, Centers for Disease Control and Prevention, US Department of Health and Human Services. 2003. Fast stats A to Z: leading causes of death. Accessed April 12, 2007, at <http://www.cdc.gov/nchs/fastats/lcod.htm>.
3. North, K. E., B. V. Howard, T. K. Welty, L. G. Best, E. T. Lee, J. L. Yeh, R. R. Fabsitz, M. J. Roman, and J. W. MacCluer. 2003. Genetic and environmental contributions to cardiovascular disease risk in American Indians: the Strong Heart Family Study. *Am. J. Epidemiol.* **157**: 303–314.
4. Sing, C. F., J. H. Stengard, and S. L. Kardina. 2003. Genes, environment, and cardiovascular disease. *Arterioscler. Thromb. Vasc. Biol.* **23**: 1190–1196.
5. Brousseau, T., A. M. Dupuy-Gorce, A. Evans, D. Arveiler, J. B. Ruidavets, B. Haas, J. P. Cambou, G. Luc, P. Ducimetiere, P. Amouyel, et al. 2002. Significant impact of the highly informative (CA)<sub>n</sub> repeat polymorphism of the APOA-II gene on the plasma APOA-II concentrations and HDL subfractions: the ECTIM Study. *Am. J. Med. Genet.* **110**: 19–24.
6. Brown, M. S., and J. L. Goldstein. 1997. The SREBP pathway: regulation of cholesterol metabolism by proteolysis of a membrane-bound transcription factor. *Cell.* **89**: 331–340.
7. Bu, X., C. H. Warden, Y. R. Xia, C. De Meester, D. L. Puppione, S. Teruya, B. Lokensgard, S. Daneshmand, J. Brown, R. J. Gray, et al. 1994. Linkage analysis of the genetic determinants of high density lipoprotein concentrations and composition: evidence for involvement of the apolipoprotein A-II and cholesteryl ester transfer protein loci. *Hum. Genet.* **93**: 639–648.
8. Cases, S., S. J. Smith, Y. W. Zheng, H. M. Myers, S. R. Lear, E. Sande, S. Novak, C. Collins, C. B. Welch, A. J. Lusis, et al. 1998. Identification of a gene encoding an acyl CoA:diacylglycerol acyltransferase, a key enzyme in triacylglycerol synthesis. *Proc. Natl. Acad. Sci. USA.* **95**: 13018–13023.
9. Wang, X., M. Ria, P. M. Kelmenson, P. Eriksson, D. C. Higgins, A. Samnegard, C. Petros, J. Rollins, A. M. Bennet, B. Wiman, et al. 2005. Positional identification of TNFSF4, encoding OX40 ligand,

as a gene that influences atherosclerosis susceptibility. *Nat. Genet.* **37**: 365–372.

10. Castellani, L. W., A. Weinreb, J. Bodnar, A. M. Goto, M. Doolittle, M. Mehrabian, P. Demant, and A. J. Lusis. 1998. Mapping a gene for combined hyperlipidaemia in a mutant mouse strain. *Nat. Genet.* **18**: 374–377.
11. Purcell-Huynh, D. A., A. Weinreb, L. W. Castellani, M. Mehrabian, M. H. Doolittle, and A. J. Lusis. 1995. Genetic factors in lipoprotein metabolism. Analysis of a genetic cross between inbred mouse strains NZB/BINJ and SM/J using a complete linkage map approach. *J. Clin. Invest.* **96**: 1845–1858.
12. Pitman, W. A., M. H. Hunt, C. McFarland, and B. Paigen. 1998. Genetic analysis of the difference in diet-induced atherosclerosis between the inbred mouse strains SM/J and NZB/BINJ. *Arterioscler. Thromb. Vasc. Biol.* **18**: 615–620.
13. Wang, X., I. Le Roy, E. Nicodeme, R. Li, R. Wagner, C. Petros, G. A. Churchill, S. Harris, A. Darvasi, J. Kirilovsky, et al. 2003. Using advanced intercross lines for high-resolution mapping of HDL cholesterol quantitative trait loci. *Genome Res.* **13**: 1654–1664.
14. Suto, J., Y. Takahashi, and K. Sekikawa. 2004. Quantitative trait locus analysis of plasma cholesterol and triglyceride levels in C57BL/6J × RR F<sub>2</sub> mice. *Biochem. Genet.* **42**: 347–363.
15. Ishimori, N., R. Li, P. M. Kelmenson, R. Korstanje, K. A. Walsh, G. A. Churchill, K. Forsman-Semb, and B. Paigen. 2004. Quantitative trait loci that determine plasma lipids and obesity in C57BL/6J and 129S1/SvImJ inbred mice. *J. Lipid Res.* **45**: 1624–1632.
16. Korstanje, R., J. J. Albers, G. Wolfbauer, R. Li, A. Y. Tu, G. A. Churchill, and B. J. Paigen. 2004. Quantitative trait locus mapping of genes that regulate phospholipid transfer activity in SM/J and NZB/BINJ inbred mice. *Arterioscler. Thromb. Vasc. Biol.* **24**: 155–160.
17. Korstanje, R., R. Li, T. Howard, P. Kelmenson, J. Marshall, B. Paigen, and G. Churchill. 2004. Influence of sex and diet on quantitative trait loci for HDL cholesterol levels in an SM/J by NZB/BINJ intercross population. *J. Lipid Res.* **45**: 881–888.
18. Lyons, M. A., R. Korstanje, R. Li, K. A. Walsh, G. A. Churchill, M. C. Carey, and B. Paigen. 2004. Genetic contributors to lipoprotein cholesterol levels in an intercross of 129S1/SvImJ and RIIS/J inbred mice. *Physiol. Genomics.* **17**: 114–121.
19. Lyons, M. A., H. Wittenburg, R. Li, K. A. Walsh, G. A. Churchill, M. C. Carey, and B. Paigen. 2003. Quantitative trait loci that determine lipoprotein cholesterol levels in DBA/2J and CAST/Ei inbred mice. *J. Lipid Res.* **44**: 953–967.
20. Lyons, M. A., H. Wittenburg, R. Li, K. A. Walsh, R. Korstanje, G. A. Churchill, M. C. Carey, and B. Paigen. 2004. Quantitative trait loci that determine lipoprotein cholesterol levels in an intercross of 129S1/SvImJ and CAST/Ei inbred mice. *Physiol. Genomics.* **17**: 60–68.
21. Gu, L., M. W. Johnson, and A. J. Lusis. 1999. Quantitative trait locus analysis of plasma lipoprotein levels in an autoimmune mouse model: interactions between lipoprotein metabolism, autoimmune disease, and atherogenesis. *Arterioscler. Thromb. Vasc. Biol.* **19**: 442–453.
22. Pitman, W. A., R. Korstanje, G. A. Churchill, E. Nicodeme, J. J. Albers, M. C. Cheung, M. A. Staton, S. S. Sampson, S. Harris, and B. Paigen. 2002. Quantitative trait locus mapping of genes that regulate HDL cholesterol in SM/J and NZB/BINJ inbred mice. *Physiol. Genomics.* **9**: 93–102.
23. Singer, J. B., A. E. Hill, L. C. Burrage, K. R. Olszens, J. Song, M. Justice, W. E. O'Brien, D. V. Conti, J. S. Witte, E. S. Lander, et al. 2004. Genetic dissection of complex traits with chromosome substitution strains of mice. *Science.* **304**: 445–448.
24. Suto, J., and K. Sekikawa. 2003. Quantitative trait locus analysis of plasma cholesterol and triglyceride levels in KK × RR F<sub>2</sub> mice. *Biochem. Genet.* **41**: 325–341.
25. York, B., K. Lei, and D. B. West. 1996. Sensitivity to dietary obesity linked to a locus on chromosome 15 in a CAST/Ei × C57BL/6J F<sub>2</sub> intercross. *Mamm. Genome.* **7**: 677–681.
26. Wang, X., and B. Paigen. 2005. Genetics of variation in HDL cholesterol in humans and mice. *Circ. Res.* **96**: 27–42.
27. Wang, X., and B. Paigen. 2002. Quantitative trait loci and candidate genes regulating HDL cholesterol: a murine chromosome map. *Arterioscler. Thromb. Vasc. Biol.* **22**: 1390–1401.
28. Srivastava, A. K., S. Mohan, G. L. Masinde, H. Yu, and D. J. Baylink. 2006. Identification of quantitative trait loci that regulate obesity and serum lipid levels in MRL/MpJ × SJL/J inbred mice. *J. Lipid Res.* **47**: 123–133.

29. Li, R., M. A. Lyons, H. Wittenburg, B. Paigen, and G. A. Churchill. 2005. Combining data from multiple inbred line crosses improves the power and resolution of quantitative trait loci mapping. *Genetics*. **169**: 1699–1709.
30. Jagodic, M., and T. Olsson. 2006. Combined-cross analysis of genome-wide linkage scans for experimental autoimmune encephalomyelitis in rat. *Genomics*. **88**: 737–744.
31. Wittenburg, H., M. A. Lyons, R. Li, U. Kurtz, X. Wang, J. Mossner, G. A. Churchill, M. C. Carey, and B. Paigen. 2006. QTL mapping for genetic determinants of lipoprotein cholesterol levels in combined crosses of inbred mouse strains. *J. Lipid Res.* **47**: 1780–1790.
32. Wergedal, J. E., C. L. Ackert-Bicknell, S. W. Tsaih, M. H. Sheng, R. Li, S. Mohan, W. G. Beamer, G. A. Churchill, and D. J. Baylink. 2006. Femur mechanical properties in the F2 progeny of an NZB/B1NJ  $\times$  RF/J cross are regulated predominantly by genetic loci that regulate bone geometry. *J. Bone Miner. Res.* **21**: 1256–1266.
33. Sugiyama, F., G. A. Churchill, D. C. Higgins, C. Johns, K. P. Makaritsis, H. Gavras, and B. Paigen. 2001. Concordance of murine quantitative trait loci for salt-induced hypertension with rat and human loci. *Genomics*. **71**: 70–77.
34. Sen, S., and G. A. Churchill. 2001. A statistical framework for quantitative trait mapping. *Genetics*. **159**: 371–387.
35. Dansky, H. M., P. Shu, M. Donavan, J. Montagno, D. L. Nagle, J. S. Smutko, N. Roy, S. Whiteing, J. Barrios, T. J. McBride, et al. 2002. A phenotype-sensitizing Apoe-deficient genetic background reveals novel atherosclerosis predisposition loci in the mouse. *Genetics*. **160**: 1599–1608.
36. Brockmann, G. A., J. Kratzsch, C. S. Haley, U. Renne, M. Schwerin, and S. Karle. 2000. Single QTL effects, epistasis, and pleiotropy account for two-thirds of the phenotypic F(2) variance of growth and obesity in DU6i  $\times$  DBA/2 mice. *Genome Res.* **10**: 1941–1957.
37. Schriml, L. M., and M. Dean. 2000. Identification of 18 mouse ABC genes and characterization of the ABC superfamily in *Mus musculus*. *Genomics*. **64**: 24–31.
38. Tominaga, K., C. Kondo, T. Kagata, T. Hishida, M. Nishizuka, and M. Imagawa. 2004. The novel gene fad158, having a transmembrane domain and leucine-rich repeat, stimulates adipocyte differentiation. *J. Biol. Chem.* **279**: 34840–34848.
39. Topham, M. K., and S. M. Prescott. 1999. Mammalian diacylglycerol kinases, a family of lipid kinases with signaling functions. *J. Biol. Chem.* **274**: 11447–11450.
40. Paigen, B., P. A. Holmes, E. K. Novak, and R. T. Swank. 1990. Analysis of atherosclerosis susceptibility in mice with genetic defects in platelet function. *Arteriosclerosis*. **10**: 648–652.
41. Welch, C. L., Y. R. Xia, I. Shechter, R. Farese, M. Mehrabian, S. Mehdizadeh, C. H. Warden, and A. J. Lusis. 1996. Genetic regulation of cholesterol homeostasis: chromosomal organization of candidate genes. *J. Lipid Res.* **37**: 1406–1421.
42. Pan, Y., W. K. Decker, A. H. Huq, and W. J. Craigen. 1999. Retrotransposition of glycerol kinase-related genes from the X chromosome to autosomes: functional and evolutionary aspects. *Genomics*. **59**: 282–290.
43. Ishimori, N., R. Li, K. A. Walsh, R. Korstanje, J. A. Rollins, P. Petkov, M. T. Pletcher, T. Wiltshire, L. R. Donahue, C. J. Rosen, et al. 2006. Quantitative trait loci that determine BMD in C57BL/6J and 129S1/SvImJ inbred mice. *J. Bone Miner. Res.* **21**: 105–112.
44. Miyazaki, M., Y. C. Kim, M. P. Gray-Keller, A. D. Attie, and J. M. Ntambi. 2000. The biosynthesis of hepatic cholesterol esters and triglycerides is impaired in mice with a disruption of the gene for stearoyl-CoA desaturase 1. *J. Biol. Chem.* **275**: 30132–30138.
45. Brown, A. C., W. I. Olver, C. J. Donnelly, M. E. May, J. K. Naggert, D. J. Shaffer, and D. C. Roopenian. 2005. Searching QTL by gene expression: analysis of diabetes. *BMC Genet.* **6**: 12.
46. Westerberg, R., J. E. Mansson, V. Golozoubova, I. G. Shabalina, E. C. Backlund, P. Tvrdik, K. Retterstol, M. R. Capecchi, and A. Jacobsson. 2006. ELOVL3 is an important component for early onset of lipid recruitment in brown adipose tissue. *J. Biol. Chem.* **281**: 4958–4968.
47. Xu, H., D. Wilcox, P. Nguyen, M. Voorbach, T. Suhar, S. J. Morgan, W. F. An, L. Ge, J. Green, Z. Wu, et al. 2006. Hepatic knockdown of mitochondrial GPAT1 in ob/ob mice improves metabolic profile. *Biochem. Biophys. Res. Commun.* **349**: 439–448.
48. Machleder, D., B. Ivandic, C. Welch, L. Castellani, K. Reue, and A. J. Lusis. 1997. Complex genetic control of HDL levels in mice in response to an atherogenic diet. Coordinate regulation of HDL levels and bile acid metabolism. *J. Clin. Invest.* **99**: 1406–1419.
49. Schuster, G. U., L. Johansson, S. Kietz, T. M. Stulnig, P. Parini, and J. A. Gustafsson. 2006. Improved metabolic control by depletion of liver X receptors in mice. *Biochem. Biophys. Res. Commun.* **348**: 176–182.
50. Forte, T. M., M. N. Oda, L. Knoff, B. Frei, J. Suh, J. A. Harmony, W. D. Stuart, E. M. Rubin, and D. S. Ng. 1999. Targeted disruption of the murine lecithin:cholesterol acyltransferase gene is associated with reductions in plasma paraoxonase and platelet-activating factor acetylhydrolase activities but not in apolipoprotein J concentration. *J. Lipid Res.* **40**: 1276–1283.
51. Langner, C. A., E. H. Birkenmeier, O. Ben-Zeev, M. C. Schotz, H. O. Sweet, M. T. Davison, and J. I. Gordon. 1989. The fatty liver dystrophy (fld) mutation. A new mutant mouse with a developmental abnormality in triglyceride metabolism and associated tissue-specific defects in lipoprotein lipase and hepatic lipase activities. *J. Biol. Chem.* **264**: 7994–8003.
52. Peterfy, M., J. Phan, and K. Reue. 2005. Alternatively spliced lipin isoforms exhibit distinct expression pattern, subcellular localization, and role in adipogenesis. *J. Biol. Chem.* **280**: 32883–32889.
53. Vikramadithyan, R. K., K. Hirata, H. Yagyu, Y. Hu, A. Augustus, S. Homma, and I. J. Goldberg. 2005. Peroxisome proliferator-activated receptor agonists modulate heart function in transgenic mice with lipotoxic cardiomyopathy. *J. Pharmacol. Exp. Ther.* **313**: 586–593.